Chapter 12

Vascular and Cardiac CT in Small Animals

Giovanna Bertolini and Luca Angeloni

Additional information is available at the end of the chapter

http://dx.doi.org/10.5772/intechopen.69848

Abstract

Computed tomography (CT) is increasingly available in veterinary practice. As for humans, CT has a tremendous potential in various clinical scenario. Oncology and traumatized dogs and cats are probably the veterinary patients that get more benefit from new CT applications. However, the most amazing progresses are in vascular and cardiac applications. The advent and rapid diffusion of advanced scanner technology (multidetector row) offer unparalleled diagnostic opportunity in daily practice for comprehensive evaluation of complex cardiovascular diseases. New skills and knowledge are necessary for radiologists and nonradiologists for understanding this revolutionary field of radiology.

Keywords: CT angiography, cardiac CT, vascular anomalies, portosystemic shunt, vascular ring anomalies, cardiac diseases

1. Introduction

Computed tomography (CT) is a cross-sectional imaging modality based on the absorption of X-rays in the patient. The overall performance of a CT system depends on several key components, comprising the X-ray source, a high-powered current generator, number of detectors, detector electronics, data transmission systems, and the computer system for image pre and post processing [1]. CT angiography (CTA) first became possible with the advent of spiral CT in the early 1980s, which combined simultaneous continuous gantry rotation and table movement, succeeding the axial or step-and-shoot acquisition mode of conventional CT scanners [2, 3]. In this manner, the tube-detector system takes a helical or spiral path around the patient moving through the gantry while the detectors collect the data. The *x*-*y* plane is the plane of the slice, whereas the *z* direction is along the axis of the patient (**Figure 1**).

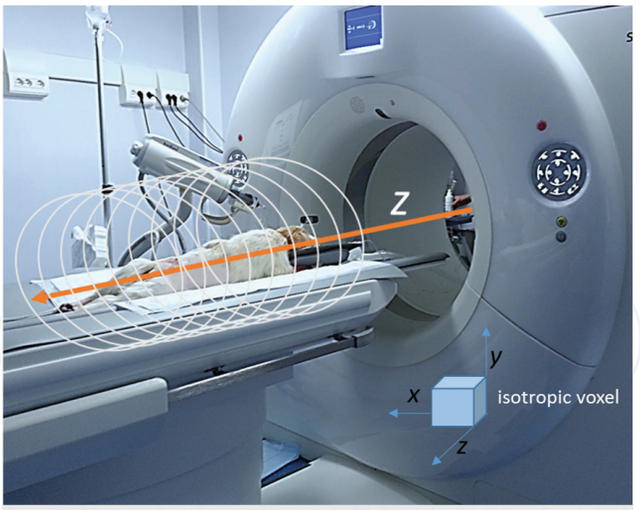

- x-y resolution (in plane resolution)
  - FOV/matrix size
  - Kernel (reconstruction algorithm)
- z-axis resolution (longitudinal resolution)
  - Slice widht
  - Reconstruction overlap (i.e. 50%)

Figure 1. Schematization of in plane, longitudinal resolution, and isotropic voxel.

The scan volume is composed of thousands of volume elements (voxels). Ideally, for high-quality images, voxels should be of equal dimensions in all three spatial axes (*x*-*y*-*z*), so that the spatial resolution is isotropic, which means equal in all directions.

The *isotropic resolution* is a fundamental prerequisite for high-quality vascular studies and post-processing reconstruction. The *temporal resolution* is the second essential requirement for vascular and cardiac CT studies. Larger volume coverage with isotropic resolution and high temporal resolution (fast scanning) was not possible using single-detector spiral CT. For this, at the end of the 1990s, all major manufacturers introduced the first generation of (MDCT) systems, having 4 rows of detectors and systems with 8, 10, and 16 detector arrays became available after few years. The 4- and 8-slice systems still showed inherent limitations regarding scan times and had limited *z*-axis resolution (with fully isotropic acquisition being possible for limited body volume). The advent of 16-MDCT scanners in 2001 represented a breakthrough in medical imaging, allowing routine scanning of larger volumes with true isotropic, submillimeter spatial resolution. 16-MDCT transformed CT from a transaxial cross-sectional technique into a truly three-dimensional (3D) imaging modality. This technology, still largely available in veterinary practice, has been overwhelmed in human field and in most advanced veterinary centers by newer CT scanners with 64, 128, 256, and 320 detector rows. Compared with 4-MDCT scanners, the performance of 64-MDCT scanners has increased more than 20 times, due to the increase in the number of detector rows and rotation [4]. The most recent dual-source CT scanner (DSCT), which features two tube-detector arrays, can achieve a rotation time of up to 0.25 s and a volume coverage speed of up to 737 mm/s [5]. Voluntary breath holding is not possible in veterinary patients as it is in conscious adult human patients. Thus, veterinary patients are usually anesthetized and intubated

during the scans. The reduced data acquisition time of faster MDCT scanners and DSCT results in shorter anesthesia or, in selected cases, in decreased need of anesthesia.

2. Principles of MDCT angiography

The simultaneous acquisition of several sections not only results in an extremely increased scan speed but also in an extension of the CT scan range with isotropic resolution, which allow for reconstructing images in any arbitrary plane without loss of image quality. When properly used, MDCT scanners can provide high-quality three-dimensional (3D) mapping of the vasculature, allowing simultaneous evaluation of the vascular lumen, as well as the vessel wall and surrounding structures. Contrast medium (CM) is essential for CT angiography (CTA). In our patients, CM is usually injected through an intravenous catheter placed in a peripheral vein. When injected, CM reaches the heart and then travels throughout the body in the cardiovascular circulation. The goal of CTA is to achieve adequate opacification (magnitude of contrast enhancement) in the vascular territory of interest, within a certain time (timing of CM), and to maintain a consistent level of enhancement throughout scanning (shaping of CM) [6, 7]. CM concentration and injection protocol need to be adapted to the patient characteristics, the vascular territory of interest, and to take advantage of the capabilities of the MDCT scanner used. Intravascular attenuation of at least 300–400 HU along the full longitudinal extent of the target vasculature and throughout the duration of acquisition is considered to be a prerequisite for high-quality CTA. Vascular contrast enhancement is influenced by various interacting factors: (1) patient-related factors, (2) CM-related factors, and (3) MDCT scanner-related factors.

Principal patient factors that affect vascular enhancement are cardiac output and body weight. Veterinary patients have wide ranges of body weight and heartbeat. Thus, when designing a CTA protocol, it is essential to consider these characteristics to achieve high-quality results consistently [8, 9]. In particular, the body weight is the most important patient-related factor affecting the magnitude of contrast enhancement in vascular studies (they are inversely related). Interindividual variability in vascular contrast enhancement may be reduced by adjusting the overall iodine dose (by increasing CM volume and/or iodine concentration) and by increasing the injection rate proportional to body weight. The timing of CM is influenced by the cardiac output (inversely related). In patients with normal cardiac output, peak arterial contrast enhancement is achieved shortly after CM injection. In patients with decreased cardiac output, CM is distributed and clears slowly, leading to delayed and persistent peak arterial enhancement. In patients with higher cardiac output (small/toy breeds and cats or larger patients with diseases such as anemia or sepsis), CM distribution is unpredictable. A fixed scan delay is not recommended for CTA in veterinary patients.

Two methods are possible to predict how CM will behave in a given patient (injection individualization): (1) test bolus and (2) automated bolus triggering or bolus tracking. For the test bolus method, a small amount of CM is injected and multiple low-dose nonincremental scans are taken over the region of interest (ROI) until the contrast is visualized in the selected vessel. For first generations of MDCT scanners (4–8 MDCT), this time can be used directly as the scanning delay for subsequent CTA. When using faster MDCT scanners, however, an

additional time must be calculated to obtain a diagnostic delay, considering the scan speed, to not "outrun" the CM bolus. Using bolus-triggering technique, test bolus injection is not necessary. All state-of-art MDCT systems feature this option. Multiple images are obtained over the ROI in a nonincremental manner during CM injection and the scan is initiated automatically when the density within the vessel exceeds a predetermined Hounsfield unit (HU) value.

A mechanical power injector is essential for MDCT angiography. This device allows preprogramming of the CM volume and flow rate and the setting of an injection pressure limit. Injection protocol parameters that may influence the opacification of target vessels are (1) injection duration (volume:rate), (2) rate of injection, and (3) volume of CM injected (duration × rate). In particular, arterial enhancement depends on the flow rate (mL/s). When the whole CM bolus is delivered at a constant injection rate (uniphasic injection), there is an upslope and downslope of the CM distribution curve and the vascular enhancement may be not uniform during volume acquisition [10, 11]. This characteristic is less important for short scan ranges (e.g., CTA of the liver, pancreas, etc.) or with newer fast scanners, but may be problematic when scanning larger vascular territories (e.g., aortoiliac CTA) or using slower CT scanners. Biphasic injection (a rapid phase, followed by a second slower phase) and multiphasic, exponentially decelerating techniques (multiphasic-rate injection bolus with exponentially decreasing rate) provide more uniform enhancement with a longer plateau phase and may be indicated for larger volume coverage using slow scanners. In our experience, saline flushing following uniphasic CM bolus using same rate and of half-to-same volume (using a dual-barrel injector system) effectively improves contrast distribution in the vascular system during acquisition.

3. MDCTA of vascular diseases

MDCT has brought about dramatic changes in veterinary vascular imaging during the past decade, leading to once unconceivable noninvasive diagnostic possibilities. Nowadays, CT-angiography is reported to be the method of choice for *in vivo* vascular anatomy depiction and for the diagnosis of various vascular pathological conditions [12–15]. A wide spectrum of vascular thoracic and abdominal disorder may be studied with MDCT angiography. MDCT angiographic studies are frequently used for detailed assessment and interventional planning in case of congenital and acquired vascular thoracic or abdominal anomalies. Other indications for MDCTA include vascular thrombosis and trauma.

3.1. Thoracic CTA applications

The thoracic vascularization includes systemic vasculature and pulmonary vessels. Systemic arterial thoracic vasculature is provided by branches of the thoracic aorta. The pulmonary arteries supply 99% of the blood flow to the lungs and participate in gas exchange at the alveolar capillary membrane, while the bronchial branches of the bronchoesophageal artery supply the supporting structures of the lungs, including the pulmonary arteries. The pulmonary and bronchial arteries have rich and complex anastomoses at the capillary level. The venous drainage of the thorax is provided by cranial vena cava and azygos vein system. CM distribution after peripheral intravenous injection differs among the heart and the systemic and pulmonary arteries and veins,

and this should be considered when designing a CT protocol. The delay between the start of CM injection and the initiation of scanning should be tailored based on scanner performance and the patient's characteristics (using the bolus test or the bolus tracking technique, as said before). The ROI will be placed on different vascular structures, the aorta, or the main pulmonary artery, depending on the clinical purpose. Clinical indications for MDCTA of the thorax include anomalies of the aortic arch and its branches, bronchial and bronchoesophageal arterial anomalies, and systemic thoracic veins diseases [16–18]. Pulsatile artifacts are critical for the accurate diagnosis of aortic arch anomalies, especially in small veterinary patients. With slower 8–16-MDCT scanners, acquisition of near-isotropic dataset with spiral acquisition mode and a half-scan interpolation reconstruction (50% overlap) algorithm aid the distinction between motion artifacts and intrinsic disease. Scanners with 40 or more rows can routinely imaging of the thoracic aorta using electrocardiogram (ECG) gating. At our center, which is equipped currently with a second-generation DSCT scanner, all CT examinations of patients with suspected or known aortic arch pathologies or other cardiovascular anomalies are now ECG-gated or acquired in sub-second flash spiral mode, resulting in the freezing of cardiovascular and respiratory motions.

Most vascular ring anomalies found in dogs are *persistent right aortic arch* (PRAA) with left-sided ligamentum arteriosum, with the heart base making up the ventral portion of the ring. PRAA has been described associated with patent ductus arteriosus (PDA). One-third of dogs with PRAA also have an *aberrant left subclavian artery* that may take a retroesophageal position, contributing to esophageal compression. The *right aberrant subclavian artery* arises from the normally left-sided aortic arch, distal to the left subclavian artery, or from a bisubclavian trunk is generally reported incidentally (**Figure 2**).

Enlarged bronchial branches of bronchoesophageal artery (*bronchoesophageal artery hypertrophy (BEAH)*) and other nonbronchial thoracic arteries (e.g., intercostal, internal mammary, and inferior phrenic arteries) are frequently observed in patients with chronic pulmonary embolism. These vessels respond to chronic pulmonary ischemia and decreased pulmonary blood flow with hypertrophy or enlargement, trying to maintain blood flow to the affected lung and participate in gas exchange through the peripheral systemic-pulmonary arterial anastomoses. Thoracic CTA show prominent bronchial branches at the bronchial bifurcation, continuing their course along the bronchi, describing a tortuous path, and ultimately anastomose with the subsegmental pulmonary arteries (**Figure 3**).

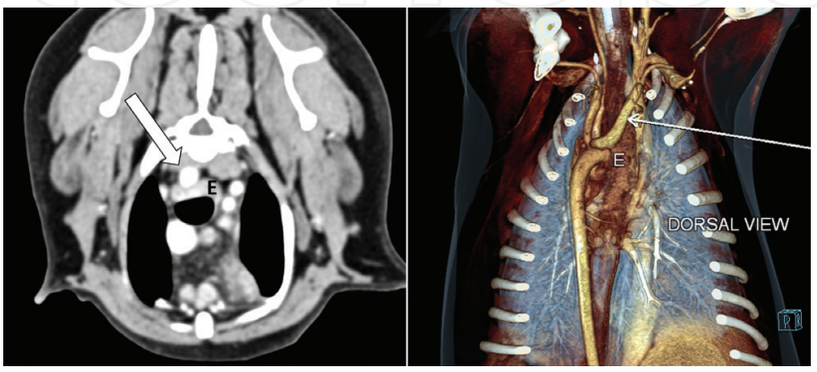

Figure 2. Right aberrant subclavian artery. E, esophagus.

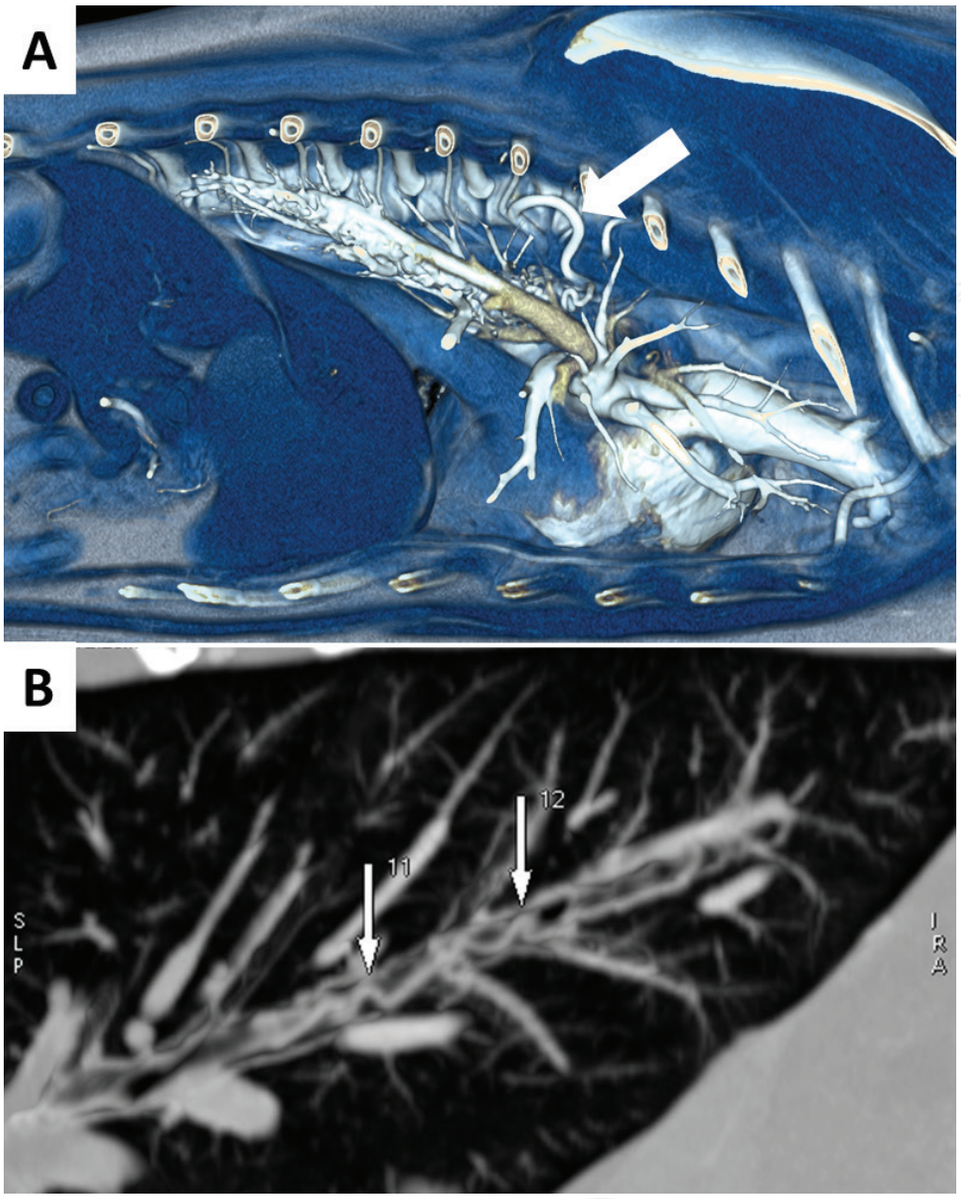

Figure 3. Acquired pattern of BEAH in a dog with chronic bronchopulmonary disease. A. Thin volume-rendered image of the thorax (the head is on the right). The arrow indicates the enlarged bronchoesophageal artery. B. Arrows indicate hypertrophied subsegmental bronchial arteries coursing along the corresponding bronchus.

Congenital pattern of BEAH is described in dogs in association with systemic-to-pulmonary fistula (with left or right main pulmonary artery) [17, 18]. This pattern might result from persistent embryonic pulmonary-systemic connection, as hypothesized for PDA. In these cases, a large vessel (5–8 mm diameter) is seen in middle mediastinum, emptying into the proximal part of the left or right pulmonary artery through a small orifice. A dense periesophageal vascular network accompanies the congenital form of BEAH (**Figure 4**).

A *persistence of the left cranial vena cava* (CrVC) is probably the most common thoracic venous anomalies in our patients [19]. Persistent left CrVC alone is often an incidental CT finding, but may cause esophageal stenosis and may be associated with severe cardiovascular defects.

http://dx.doi.org/10.5772/intechopen.69848

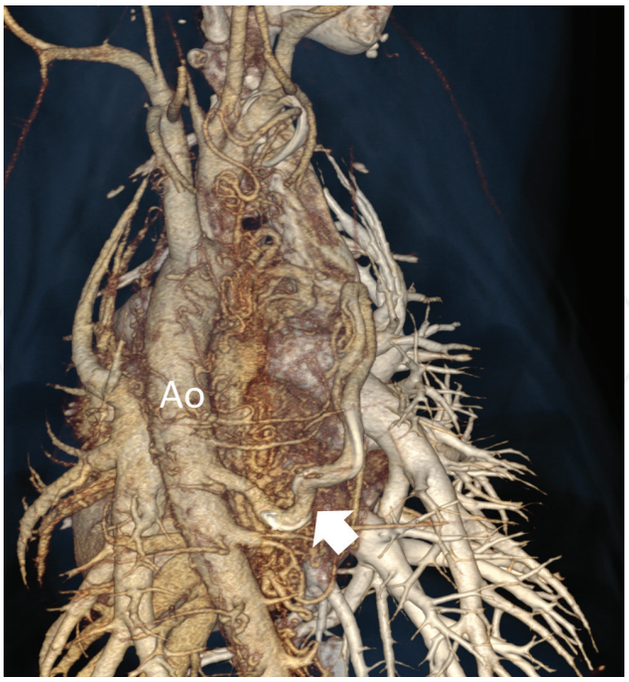

Figure 4. Congenital pattern of bronchoesophageal artery hypertrophy with artery-to-pulmonary fistula (not visible here). Note the enlarged bronchoesophageal artery arising from the thoracic aorta and the dense mediastinal vascular network (dorsal view).

The left persistent CrVC results from incomplete atrophy of the embryonic left cranial cardinal vein. Two types are described in dogs and cats: (1) a complete type, with nonatrophied left cranial cardinal vein retaining its embryological connection with the coronary sinus; (2) an incomplete type, in which the distal portion of the persistent vein atrophies, whereas the proximal portion persists and receives the hemiazygos vein.

In oncology patients, MDCTA is indicated for the assessment and interventional planning in case of mediastinal masses or tumors of the thoracic wall involving the thoracic vasculature.

3.2. Abdominal vascular diseases

Most common abdominal vascular diseases involve the caudal vena cava and the portal system. Caudal vena cava anomalies often have no or little clinical significance in themselves, but they are often associated with other vascular anomalies, such as portosystemic shunts that are clinically relevant [20–22]. In veterinary literature, MDCT angiographic studies are frequently reported for congenital portosystemic shunt assessment in dogs and cats [23–26]. Moreover, it is widely used also for the assessment of other pathological conditions of the portal system, such as acquired portal collaterals (APSS), portal vein aneurysm, and portal vein thrombosis [27–29]. Congenital anomalies of the abdominal segment of the descending aorta are rarely reported in small animals, and include variable pattern of renal arteries, aortic aneurism, and common celiacomesenteric trunk. Among acquired conditions, local thrombosis in the distal aorta with embolization to the iliac and/or femoral artery is the most common indication for MDCTA in dogs and cats (**Figure 5A**).

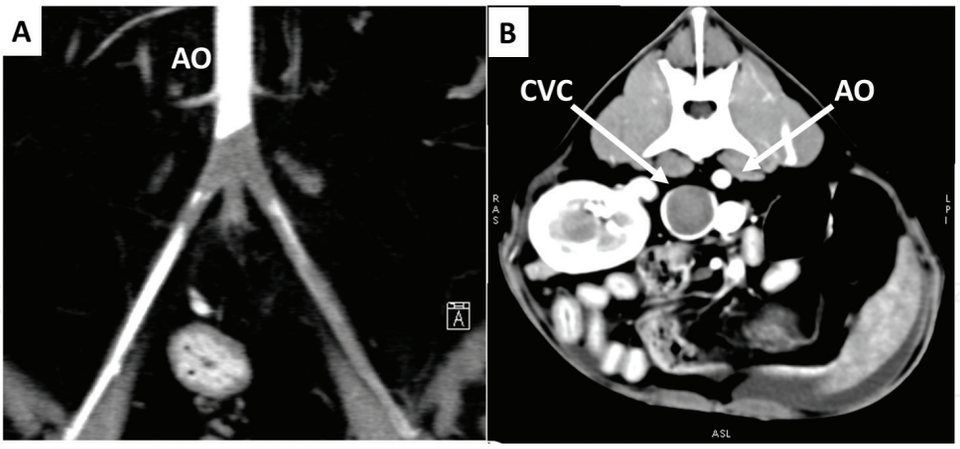

Figure 5. A. Aortoiliac thromboembolism in a dog with nephrotic syndrome. B. Caudal vena cava thrombosis in an oncologic patient (hepatic carcinoma).

The selection of an MDCTA scan protocol varies in consideration of the type of anomaly suspected and the vascular district (arterial, portal, or venous) potentially involved. For a comprehensive evaluation of the abdominal vascular structures, a multiphasic approach is necessary, including at least two vascular phases: arterial and portal venous phase that is also useful for the hepatic parenchyma evaluation. When CM is injected, opacification of the hepatic artery and its branches is encountered first, followed by the portal system, hepatic, and systemic veins. In veterinary literature, the peak aortic enhancement of normal dogs varies between 2 and 9.8 s, and peak enhancement of the portal vein varies between 14.6 and 46 s after contrast medium injection. Given the great diversity of patients' characteristics (body weight and cardiac output), the use of bolus test or automatic bolus-triggering techniques for the individualization of scan delays in multiphasic MDCT examinations is needed.

A dual- or three-phase MDCT exam can provide excellent visualization of complex vascular anomalies and offer a comprehensive overview of the entire portal system and related parenchymal organs. Various new congenital and acquired phenotypes of portosystemic collaterals have been described using MDCT technology [24–26, 30] (**Figures 6** and **7**). Good opacification of the portal venous system allows detection of endoluminal filling defects in case of portal vein thrombosis and simultaneous assessment of secondary portal collaterals (portosystemic and/or portoportal collateral vessels) (**Figure 8**).

A third vascular phase, corresponding to the interstitial hepatic phase, allows optimal visualization of systemic veins, which is essential for the evaluation of venous thrombosis and vascular invasion (**Figure 5B**). Most caudal segments of the caudal vena cava are prone to congenital variation, which is generally clinically silent themselves (**Figure 9**), but are often associated with CPSS or other vascular and nonvascular anomalies that can be of great clinical relevance.

The arterial phase is useful for detection of high-flow vascular connections (arteriovenous fistula) at any level of the body. MCDTA images show enlarged, tortuous arteries, and premature

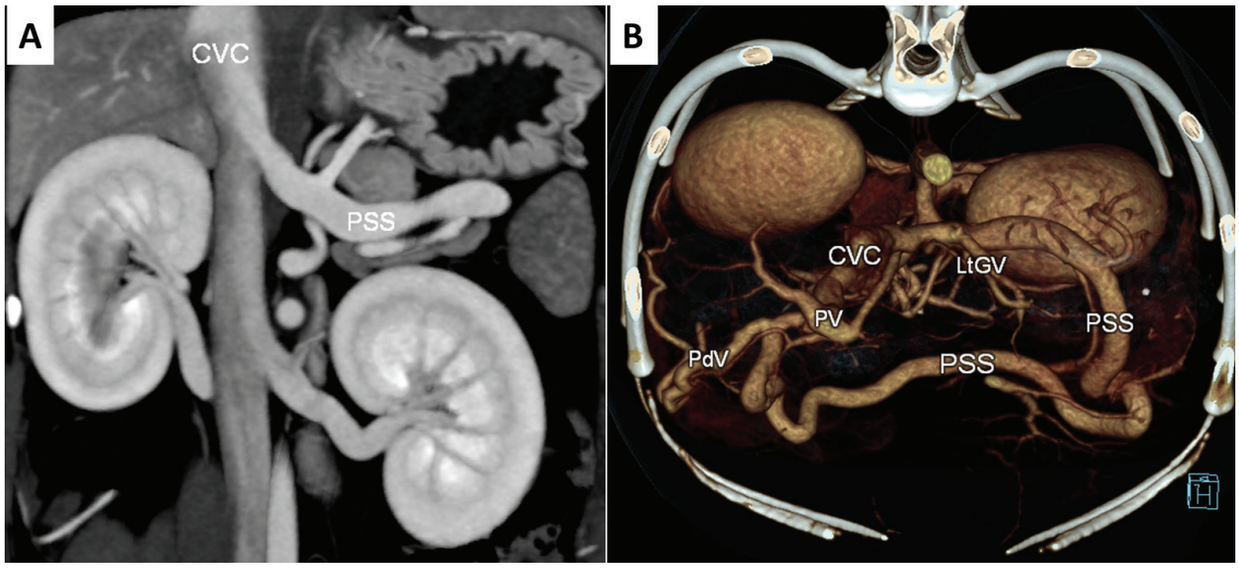

Figure 6. Extrahepatic congenital portosystemic shunt, in which the left gastric vein (LtGV) and the splenic vein had no communication with the portal vein (PV). Both veins join the anomalous vessel (PSS) that empty in the caudal vena cava (CVC). A. Dorsal thin-MIP (maximum intensity projection) showing the end of PSS into the CVC. B. Volume-rendered, frontal view showing the course of the PSS.

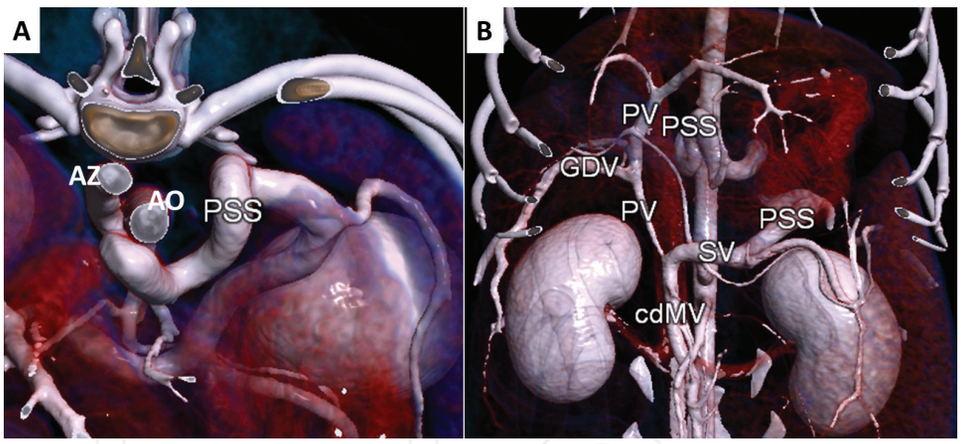

Figure 7. Congenital extrahepatic PSS between the left gastric vein and the right azygos vein. A. Volume-rendered image, frontal view. Ao, aorta, Az, azygos vein. B. Volume rendered ventral view. PV, portal vein; GDV, gastroduodenal vein; SV, splenic vein; cdMV, caudal mesenteric vein. PSS, portosystemic shunt.

filling of the veins (**Figure 10**). In the liver, an early arterial phase can reveal complex hepatic arteriovenous malformations (HAVM) that are congenital anomalous connections between branches of the hepatic artery and hepatic portal vessels.

In traumatized patients, active bleeding due to arterial or venous vascular injuries can be revealed by CM extravasation in the arterial and portal venous phases. In oncology patients, a three-phase MDCT abdominal examination provides useful information of vascular blood supply of tumors and local vascular invasion, allowing detailed interventional and surgical planning.

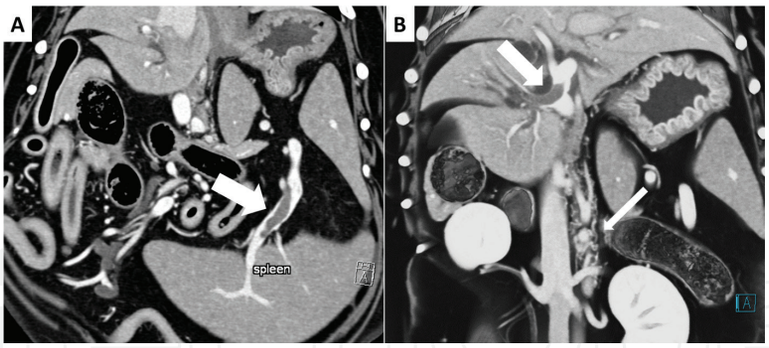

Figure 8. Portal venous phase in dogs with thrombosis of the portal system. A. The arrow indicates a filling defect in the splenic vein. B. Large arrow indicates a large filling defect in intrahepatic portal branches. The thin arrow shows some retroperitoneal varices, due to portal hypertension.

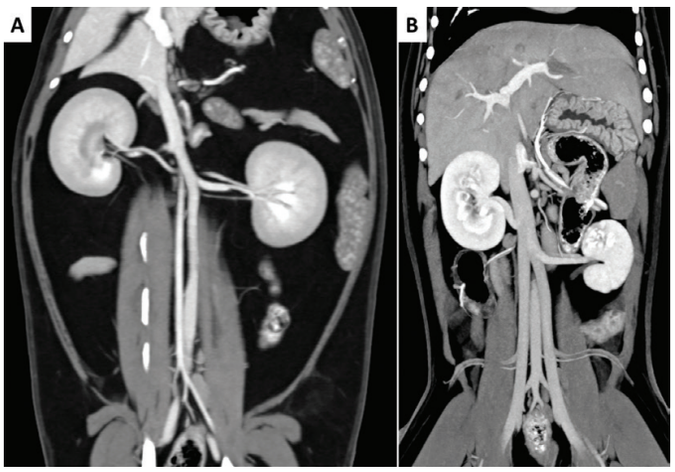

Figure 9. A. Dorsal MPR in a cat. The prerenal segment of the CVC is left sided (persistent left supracardinal vein and anomalous regression of the right one). B. Duplication of the prerenal segment of the CVC (partial duplication for persistent left supracardinal vein).

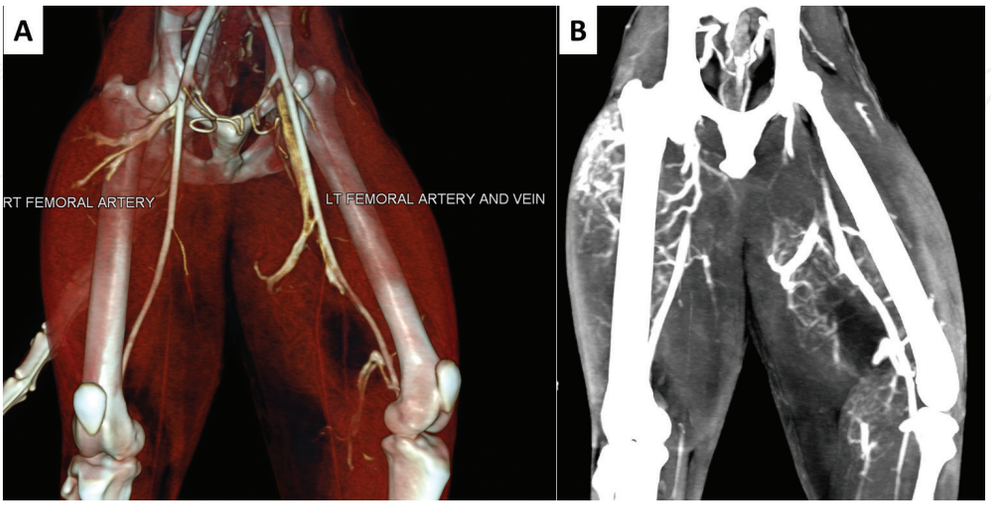

Figure 10. Peripheral arteriovenous communications in a dog. A. Volume rendering of arterial phase. Note the early enhancement of the left femoral vein. B. MIP of same volume, showing several small tortuous vessels in both legs and the muscular swelling.

4. Cardiac CT

In humans, since the advent of advanced scanner technology having 64 or more detectors, the heart and coronary arteries are routinely imaged as a motion-free volume of data. Most recent MDCT and DSCT scanners can obtain a true volumetric data set of the entire heart and adjacent structures that can be reconstructed at any point in the cardiac cycle, making CT an important imaging modality for the comprehensive assessment of cardiac morphology and function. While echocardiography remains the first-line imaging modality, CT has become an increasingly utilized complementary imaging modality for assessment of coronary and non-coronary cardiac structures, including the cardiac chamber and valves, the pulmonary arteries and veins, the thoracic aorta and its proximal branches, the cardiac veins, and the pericardium.

Cardiac CT was first described in veterinary literature in 2011 for canine coronary artery assessment using a 64-MDCT scanner [31]. Later, other studies have been published describing morphological characteristics of various cardiac structures and comparing echocardiography, magnetic resonance (MR) and CT measurements [32, 33]. As for humans, cardiac CT in veterinary patients has now become an increasingly utilized modality for the assessment of cardiac congenital conditions, cardiac and paracardiac masses, and pericardial diseases [34–36]. In clinical practice, morphological evaluation of these conditions is generally performed with non-ECG-gated CT protocols, as a part of a thoracic CT examination. Most recent MDCT is not only fast but also has high spatial and temporal resolutions, multiplanar reconstruction (MPR) capabilities, and a wide field of view, which provides information of the heart, mediastinum, and adjacent structures, including the lungs. A non-ECG-gated CT examination, however, is not a reliable way for comprehensive evaluation of small cardiac structures (e.g., coronary arteries and valves), congenital heart diseases, cardiac sizes and in many other clinical situations using first generation of MDCT scanners (≤64 rows) [32, 33]. With most advanced MDCT scanners (e.g., 128–320 detector rows) and DSCT technology, it is possible to obtain high-resolution, submillimetric data in a few seconds, providing excellent morphological detail of the heart and paracardiac structures, having minimal or no motion artifacts. For instance, at our center, now equipped with a second generation of dual-source 128-slice CT systems, cardiothoracic CT examination can be performed at a high-pitch, up to 3.4 with gantry rotation time of 0.28 s and a temporal resolution of 75 ms (**Figure 11**).

4.1. Cardiac CT basic principles

For motion-free and of diagnostic value imaging of the heart, high temporal and spatial resolution are both essential, especially in veterinary patients who have variable heart rates. CT data should be assessed during certain phases of the cardiac cycle with little cardiac motion. Ideally, a complete data set of the whole heart would be acquired within a single phase of the cardiac cycle without movement. Two methods are possible for virtually freezing the heart: prospective gating with sequential or step-and-shoot scanning mode and retrospective ECG gating (spiral) [37, 38].

In *prospective ECG-triggered sequential CT-scanning* using partial-scan technique, the scan is synchronized to the motion of the heart in order to acquire data preferably in the diastolic phase, when cardiac motion is minimal. After every scan, the table moves by the width of the acquired scan range in the *z*-direction toward the next scan position in order to provide gap-less volume

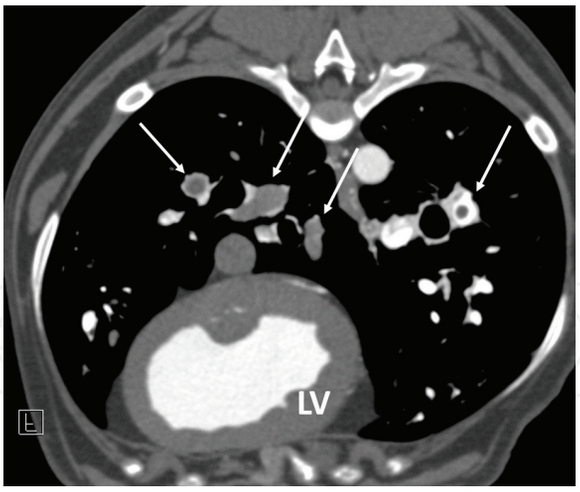

Figure 11. Non-ECG-gated, high-pitch 128-DSCT (Flash mode) of the thorax in a dog with pulmonary embolism. A transverse view. Arrows show the filling defects in pulmonary vessels, due to thrombosis. Cardiac structures are "freezed" (lv, left ventricle).

coverage (step-and-shot). The delay time for scan acquisition after an R-wave is individually based on a prospective estimation of the R-R intervals, attempting to acquire the data during the diastolic phase of the heart. Using this technique, small changes in heart rate during the sequential scan can cause acquisition in inconsistent heart phases and thus inconsistent volume coverage, resulting in artifacts at the intersections of adjacent image stacks and subsequent misregistration of lesions along *z*-axis. This may represent a limitation especially for veterinary patients, where many cardiac structures are small and complex 3D structures that require the highest possible image quality. Moreover, with prospective ECG triggering, estimation of the next R-R interval may be incorrect when heart-rate changes are present, such as in patients with arrhythmia or with a single premature ventricular contraction, which makes sections of the heart entirely uninterpretable.

In *retrospectively ECG-gated spiral scanning*, reconstructions of a continuous spiral scan are synchronized to the movement of the heart by using an ECG trace that is recorded simultaneously. The great advantage of retrospectively ECG-gated MDCT-spiral scanning is that it provides an isotropic, 3D image data set of the complete cardiac volume without gaps and misregistration of data. Retrospective ECG gating data are available during all phases of the cardiac cycle and this offers the possibility of retrospectively modifying the synchronization of the ECG trace and data reconstruction, choosing the best R-R interval for image analysis. Individual adjustment of the image-interval-position is extremely useful for imaging those patients with fast and irregular heart rate.

The scanner technology available greatly influences the scan protocol for cardiac CT evaluation. The maximum pitch in single source MDCT is usually about 1.5. Last generation of DSCT scanners allow pitch value up to 3.4. This results in maximum scan speed of 737 mm/s, which allows continuous volume coverage of a whole body in one second or less with isotropic resolution [38]. Since this impressive temporal resolution, pharmacological pretreatment for heart rate modulation is not necessary in our patients. High-detailed images of the heart can be obtained also in awake patients, independently on the heart rate. However, using

this approach, cardiac function evaluation is not possible. In our experience, low-pitch retrospective ECG-gated 128-DSCT cardiac examination performed without any pharmacological pretreatment to reduce patient's heart rate provides excellent images, useful either for morphological or functional assessments.

Factors influencing the CM hemodynamic distribution are similar to those described before for CTA. CM injection protocol should take into account the body weight and cardiac output of the patient. Both the bolus test and the bolus-triggering techniques can be used for CM injection individualization for cardiac evaluation. In standard cardiac CT for coronary artery evaluation, the ROI is placed in the ascending aorta. In this approach, the left ventricular and left atrial walls and cavities, as well as left-sided valves, will be uniformly opacified (**Figures 12** and **13**). However, depending on the contrast agent infusion protocol, the right-sided

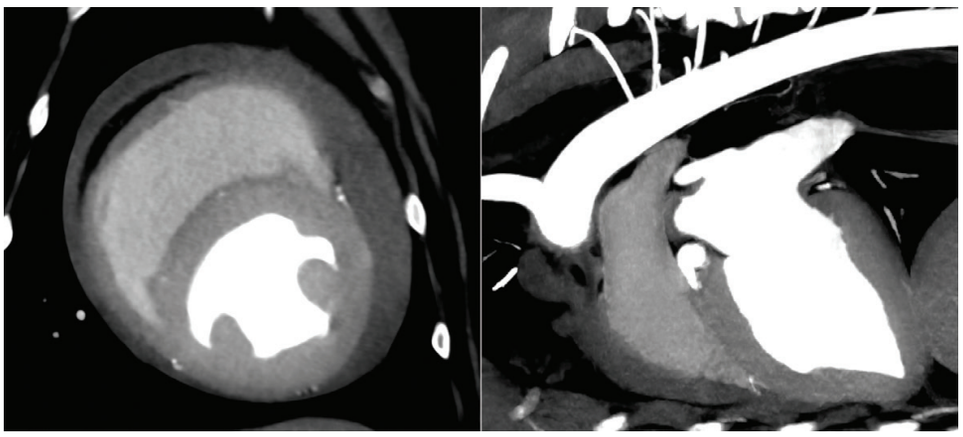

Figure 12. Retrospective ECG-gated cardiac examination with 128-DSCT (low pitch). Note the absence of motion artifacts (the patient was under general anesthesia, mechanically ventilated). The ROI has been placed on the ascending aorta (standard cardiac CT). Note the great enhancement of the aorta, left atrium, and ventricle.

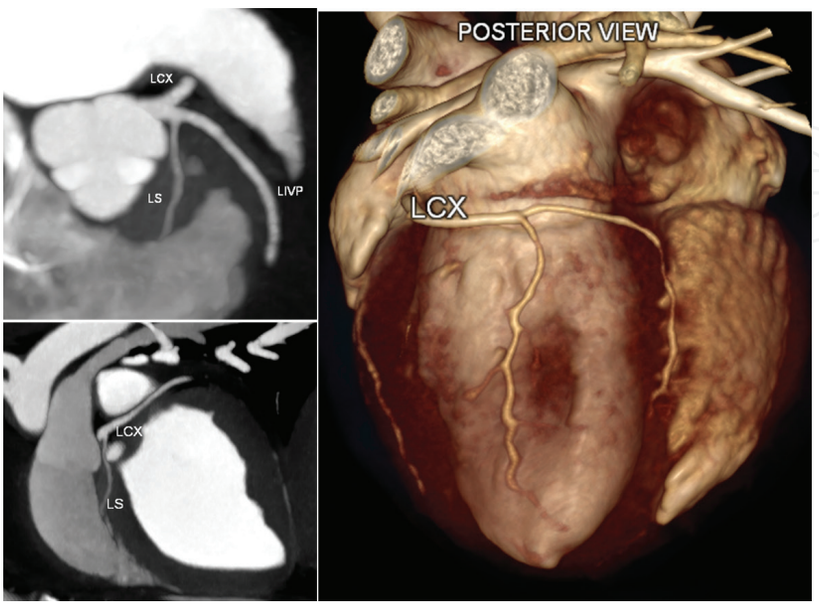

Figure 13. Retrospective ECG-gated cardiac CT in a dog (128-DSCT).

chambers, walls, and valves may or may not be suitable for interpretation. Optimal timing for right heart good opacification can be achieved placing the ROI for test bolus or bolus tracking in the main pulmonary artery. Achievement of diagnostically adequate homogeneous enhancement of the right atrium can be difficult because of mixing of unopacified blood from the caudal vena cava with high-attenuating contrast agent-opacified blood from the cranial vena cava. Streak artifacts due to high concentration of CM in the cranial vena cava or right atrium may obscure some structures or simulate the presence of masses or thrombotic lesions. Dual or triple CM bolus injection technique may lead to a more uniform opacification of right-sided cardiac structures. This may be necessary for the evaluation of patients with certain congenital heart diseases or cardiac masses.

4.2. Cardiac CT clinical applications

With ECG-gated cardiac CT examination, the anatomy of the heart is clearly depicted. MDCT is the preferred imaging modality when anomalous origin and course of coronary arteries is suspected [32, 39] (**Figure 14**). Compared to human literature, reports of congenital artery anomalies in animals are sparse, presumably because coronary artery disease is less common in veterinary patients and rarely of clinical significance, unless in the setting of pulmonary valve stenosis (PS). Further, advanced diagnostic imaging of the heart is not routinely performed, thus underestimating the frequency of coronary anomalies in our patients. ECG-gated cardiac CT allows the simultaneous evaluation of other noncoronary structures of the heart. Left and right chambers are well defined from the cardiac muscular wall and from interventricular and interatrial septum. Small structures, such as atrioventricular valves, aortic and pulmonary valves, papillary muscles of both ventricles, and trabeculae carneae are easily distinguishable [31].

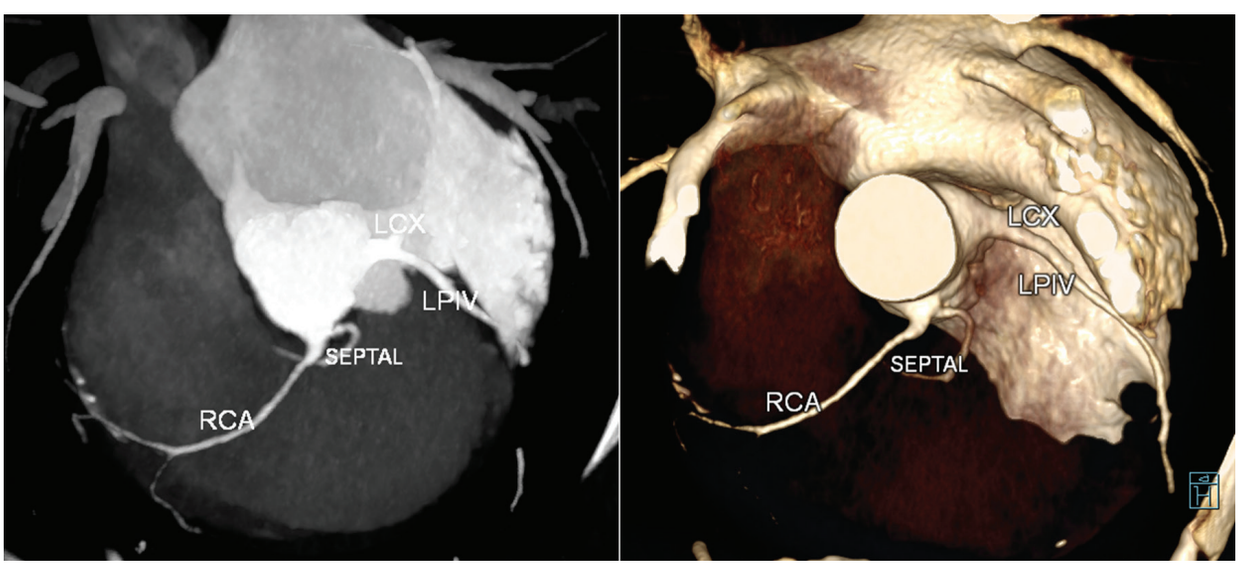

Figure 14. Retrospective ECG-gated cardiac CT in a dog with anomalous right origin of septal coronary artery branch (128-DSCT).

http://dx.doi.org/10.5772/intechopen.69848

Using retrospective ECG-gated mode with full cardiac cycle available, functional evaluations of the heart are also possible. In postprocessing, multiplanar analysis (MPR) of volume dataset allows standard planar and volumetric measurements, using same image planes normally used in echocardiography [32–35]. ECG-gated cardiac CT is also useful in patients with congenital cardiac defects such as PDA, PS, or more complex congenital heart diseases. Moreover, it is helpful for planning surgical and interventional procedures [16, 40] (**Figures 15**, **16**).

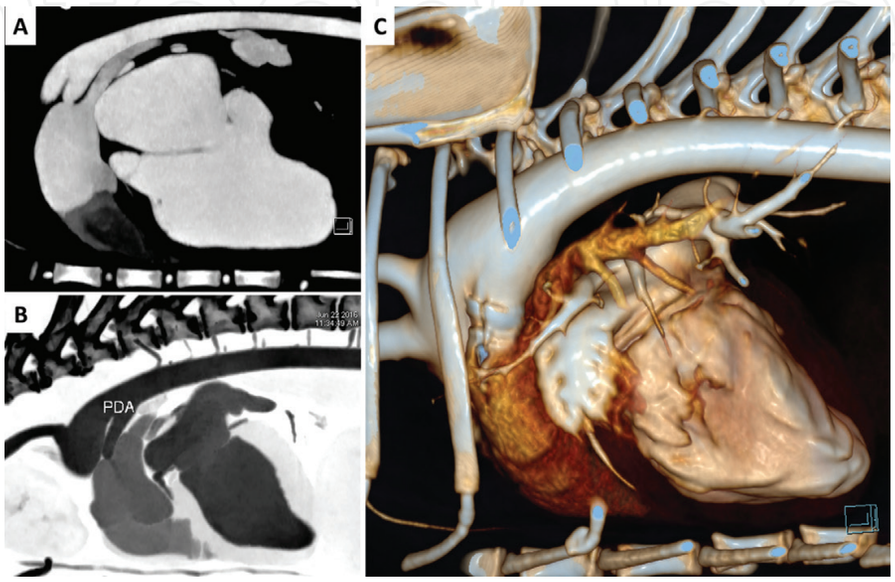

Figure 15. 128-DSCT, ECG-gated cardio CT in PDA in a dog (pre-interventional assessment) and corrected PDA with Amplatzer duct occluder (VR on the right).

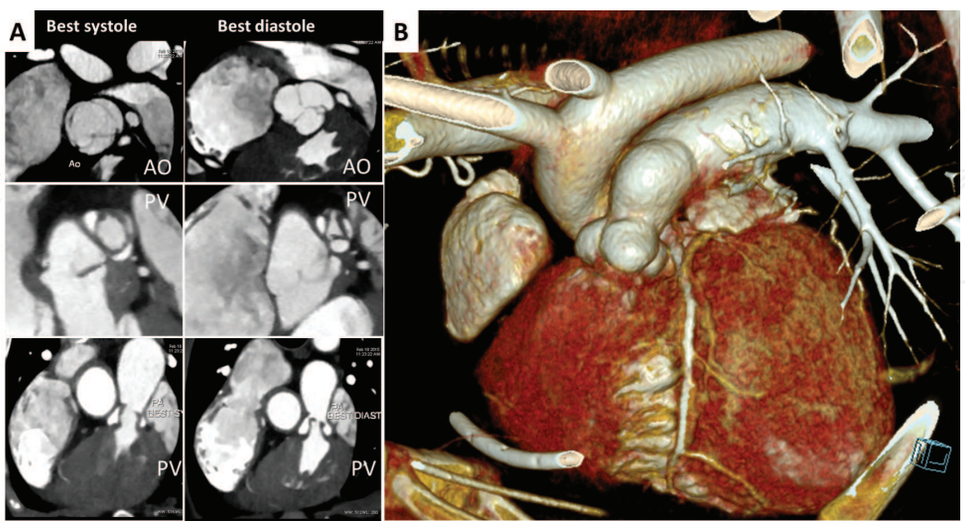

Figure 16. Retrospective ECG-gated cardiac 128-DSCT in dogs with pulmonic stenosis. A. Images on the left have been automatically reconstructed by the software in best-systolic phase and those on the right in best diastole (less motion artifacts). B. VR of another dog with pulmonic stenosis and post stenotic bulge of right ventricular outflow tract.

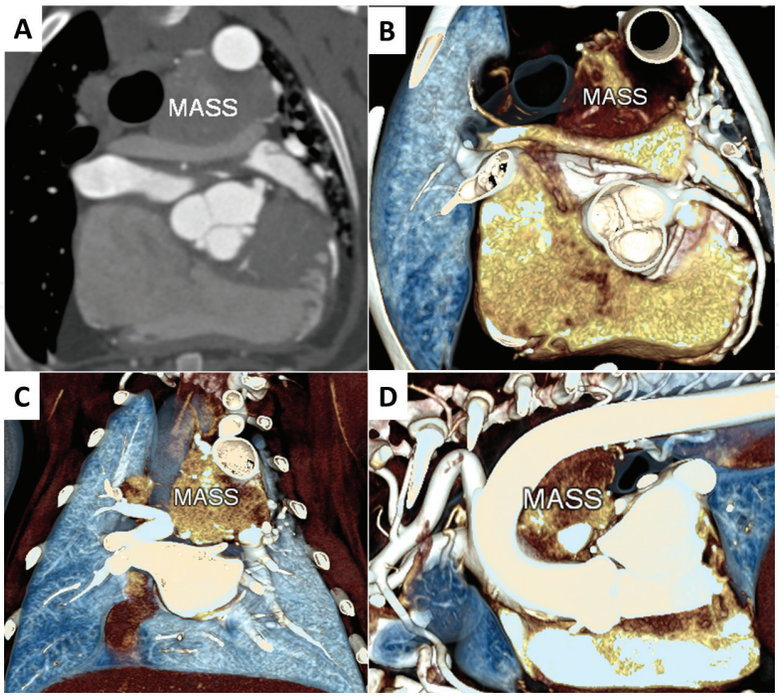

Figure 17. ECG-gated cardiothoracic examination (128-DSCT) in a dog with heart-base tumor (mass).

In clinical practice, primary or metastatic cardiac tumors can be easily identified during routine non-ECG-gated examination of the thorax. However, ECG-gated cardiac imaging in patients with suspected or known cardiac-paracardiac or pericardial tumors minimizes motion-related artifacts and allows a more precise delineation of the lesion margins (**Figure 17**).

Author details

Giovanna Bertolini* and Luca Angeloni

*Address all correspondence to: bertolini@sanmarcovet.it

Diagnostic and Interventional Radiology Division, San Marco Veterinary Clinic, Padova, Italy

References

[1] Kalender WA. X-ray computed tomography. Physics in Medicine and Biology. 2006 Jul 7;**51**(13):R29-43. Epub 2006 Jun 20. 10.1088/0031-9155/51/13/R03

[2] Flohr T, Stierstorfer K, Bruder H, Simon J, Schaller S.. New technical developments in multislice CT--Part 1: Approaching isotropic resolution with sub-millimeter 16-slice scanning. Rofo. 2002;**174**(7):839-845. DOI: 10.1055/s-2002-32692

[3] Prokop M. New challenges in MDCT. European Radiology. 2005;**15** Suppl 5:E35-E45

[4] Rogalla P, Kloeters C, Hein PA. CT technology overview: 64-slice and beyond. Radiologic Clinics of North America. 2009;**47**(1):1-11. DOI: 10.1016/j.rcl.2008.10.004

[5] Petersilka M, Bruder H, Krauss B, Stierstorfer K, Flohr TG. Technical principles of dual source CT. European Journal of Radiology. 2008;**68**(3):362-368. DOI: 10.1016/j.ejrad.2008.08.013

[6] Bae KT, Heiken JP. Scan and contrast administration principles of MDCT. European Radiology. 2005;**15** Suppl 5:E46-E59

[7] Fleischmann D, Kamaya A. Optimal vascular and parenchymal contrast enhancement: the current state of the art. Radiologic Clinics of North America. 2009;**47**(1):13-26. DOI: 10.1016/j.rcl.2008.10.009

[8] Cassel, N., Carstens, A, Becker, P. The comparison of bolus tracking and test bolus techniques for computed tomography thoracic angiography in healthy beagles. Journal of the South African Veterinary Association. 2013 May 7;**84**(1):E1-9. http://dx.doi.org/10.4102/jsava.v84i1.930

[9] Mai W, Suran JN, Cáceres AV, Reetz JA. Comparison between bolus tracking and timing-bolus techniques for renal computed tomographic angiography in normal cats. Veterinary Radiology & Ultrasound. 2013;**54**(4):343-350. DOI: 10.1111/vru.12029

[10] Lell MM, Jost G, Korporaal JG, et al. Optimizing contrast media injection protocols in state-of-the art computed tomographic angiography. Investigative Radiology. 2015;**50**(3):161-167. DOI: 10.1097/RLI.0000000000000119

[11] Apitzsch J, Jost G, Bonifer E, et al. Revival of monophasic contrast injection protocols: Superiority of a monophasic injection protocol compared to a biphasic injection protocol in high-pitch CT angiography. Acta Radiologica. 2016;**57**(10):1210-1216. DOI: 10.1177/0284185115618546

[12] Bertolini, G. MDCT for abdominal vascular assessment in dogs: MDCT basics, CT angiography, normal anatomy and congenital anomalies. Saarbrucken, Germany: Lambert Academic Publishing;2010

[13] Bertolini G, Prokop M. Multidetector-row computed tomography: technical basics and preliminary clinical applications in small animals. The Veterinary Journal. 2011;**189**(1):15-26

[14] Parry AT, White RN. Portal vein anatomy in the dog: comparison between computed tomographic angiography (CTA) and intraoperative mesenteric portovenography (IOMP). Journal of Small Animal Practice. 2015; Nov;**56**(11):657-661. DOI: 10.1111/jsap.12392

[15] De Rycke LM, Kromhout KJ, van Bree HJ, Bosmans T, Gielen IM. Computed tomography atlas of the normal cranial canine abdominal vasculature enhanced by dual-phase angiography. Anatomia, Histologia, Embryologia. 2014;**43**(6):413-422. DOI: 10.1111/ahe.12090. Epub 2013 Oct 23

[16] Henjes CR, Nolte I, Wefstaedt P. Multidetector-row computed tomography of thoracic aortic anomalies in dogs and cats: patent ductus arteriosus and vascular rings. BMC Veterinary Research. 2011;**7**:57

[17] Ledda G, Caldin M, Mezzalira G, Bertolini G. Multidetector-row computed tomography patterns of bronchoesophageal artery hypertrophy and systemic-to-pulmonary fistula in dogs. Veterinary Radiology & Ultrasound. 2015;;**56**(4):347-358. DOI: 10.1111/vru.12247

[18] LeRoux A, Granger LA,Reynolds C, Gaschen L. Computed tomography features of bronchial and non-bronchial collateral arterial circulation development in a dog diagnosed with multiple chronic pulmonary thrombi. Journal of Veterinary Cardiology. 2013;**15**:283-287

[19] Choi S-Y, Song Y-M, Lee Y-W, Choi H-J. Imaging characteristics of persistent left cranial vena cava incidentally diagnosed with computed tomography in dogs. The Journal of Veterinary Medical Science. 2016;**78**(10):1601-1606. DOI:10.1292/jvms.15-0695

[20] Bertolini G, Diana A, Cipone M, Drigo M, Caldin M. Multidetector row computed tomography and ultrasound characteristics of caudal vena cava duplication in dogs. Veterinary Radiology & Ultrasound. 2014;**55**(5):521-530. DOI: 10.1111/vru.12162

[21] Pey P, Marcon O, Drigo M, Specchi S, Bertolini G. Multidetector-row computed tomographic characteristics of presumed preureteral vena cava in cats. Veterinary Radiology & Ultrasound. 2015;**56**(4):359-366. DOI: 10.1111/vru.12251

[22] Specchi S, d'Anjou MA, Carmel EN, Bertolini G. Computed tomographic characteristics of collateral venous pathways in dogs with caudal vena cava obstruction. Veterinary Radiology & Ultrasound. 2014;**55**(5):531-538. DOI: 10.1111/vru.12167

[23] Bertolini G, Rolla EC, Zotti A, Caldin M. Three-dimensional multislice helical computed tomography techniques for canine extra-hepatic portosystemic shunt assessment. Veterinary Radiology & Ultrasound. 2006;**47**(5):439-443

[24] Nelson NC, Nelson LL. Anatomy of extrahepatic portosystemic shunts in dogs as determined by computed tomography angiography. Veterinary Radiology & Ultrasound. 2011;**52**(5):498-506. DOI: 10.1111/j.1740-8261.2011.01827.x

[25] White RN, Parry AT. Morphology of congenital portosystemic shunts emanating from the left gastric vein in dogs and cats. Journal of Small Animal Practice. 2013;**54**(9):459-67. DOI: 10.1111/jsap.12116

[26] White RN, Parry AT. Morphology of congenital portosystemic shunts involving the right gastric vein in dogs. Journal of Small Animal Practice. 2015;**56**(7):430-440. DOI: 10.1111/jsap.12355

[27] Bertolini G. Acquired portal collateral circulation in the dog and cat. Veterinary Radiology & Ultrasound. 2010;**51**(1):25-33

[28] Bertolini G, Caldin M. Computed tomography findings in portal vein aneurysm of dogs. The Veterinary Journal. 2012;**193**(2):475-480. DOI: 10.1016/j.tvjl.2011.12.002. Epub 2012 Jan 24

[29] Specchi S, Pey P, Ledda G, Lustgarten M, Thrall D, Bertolini G. Computed tomographic and ultrasonographic characteristics of cavernous transformation of the obstructed portal vein in small animals. Veterinary Radiology & Ultrasound. 2015; DOI: 10.1111/Vru.12265

[30] Fukushima K, Kanemoto H, Ohno K, Takahashi M, Fujiwara R, Nishimura R, Tsujimoto H. Computed tomographic morphology and clinical features of extrahepatic portosystemic shunts in 172 dogs in Japan. The Veterinary Journal. 2014;**199**(3):376-381. DOI: 10.1016/j.tvjl.2013.11.013

[31] Drees R, Frydrychowicz A, Reeder SB, Pinkerton ME, Johnson R. 64-multidetector computed tomographic angiography of the canine coronary arteries. Veterinary Radiology & Ultrasound?: The Official Journal of the American College of Veterinary Radiology and the International Veterinary Radiology Association. 2011;**52**(5):507-515. DOI: 10.1111/j.1740-8261.2011.01826.x

[32] Laborda-Vidal P, Maddox TW, Navarro-Cubas X et al. Comparison between echocardiographic and non-ECG-gated CT measurements in dogs. Veterinary Record. 2015;**176**(13):335. DOI: 10.1136/vr.102724. Epub 2015 Feb 18

[33] Drees R, Johnson RA, Stepien RL, Rio AMD, Saunders JH, François CJ. Quantitative planar and volumetric cardiac measurements using 64 MDCT and 3T MRI versus standard 2D and M-mode echocardiography: Does anesthetic protocol matter? Veterinary Radiology & Ultrasound?: The Official Journal of the American College of Veterinary Radiology and the International Veterinary Radiology Association. 2015;**56**(6):638-657. DOI:10.1111/vru.12269

[34] Sieslack AK, Dziallas P, Nolte I. Wefstaedt P. Comparative assessment of left ventricular function variables determined via cardiac computed tomography and cardiac magnetic resonance imaging in dogs. American Journal of Veterinary Research. 2013;**74**(7):990-998. DOI: 10.2460/ajvr.74.7.990

[35] Sieslack, A.K., Dziallas, P., Nolte, I. et al. Quantification of right ventricular volume in dogs: a comparative study between three-dimensional echocardiography and computed tomography with the reference method magnetic resonance imaging. BMC Veterinary Research. 2014;**10**:242. DOI:10.1186/s12917-014-0242-3

[36] Laborda-Vidal P., Pedro B., Baker M., et al. Use of ECG-gated computed tomography, echocardiography and selective angiography in five dogs with pulmonic stenosis and one dog with pulmonic stenosis and aberrant coronary arteries, Journal of Veterinary Cardiology. 2016;**18**(4):418

[37] Flohr T, Ohnesorge B. Cardiac gating. In: Re-my-Jardin M, Remy J, editors. Integrated Cardiothoracic Imaging with MDCT. Berlin, Germany, Springer; 2009

[38] Sun Z, Al Moudi M, Cao Y. CT angiography in the diagnosis of cardiovascular disease: a transformation in cardiovascular CT practice. Quantitative Imaging in Medicine and Surgery. 2014;**4**(5):376-396. DOI: 10.3978/j.issn.2223-4292.2014.10.02

[39] Sabel BO, Buric K, Karara N, et al. High-pitch CT pulmonary angiography in third-generation dual-source CT: Image quality in an unselected patient population. PLoS One. 2016;**11**(2):e0146949. DOI:10.1371/journal.pone.0146949

[40] Scansen BA. Coronary artery anomalies in animals. Veterinary Sciences. 2017;**4**:20. DOI:10.3390/vetsci4020020

IntechOpen